
REVCD - REVERSED CONDITIONAL DIFFUSION FOR GENERALIZED ZERO-SHOT LEARNING

A PREPRINT

William Heyden*, Habib Ullah, M. Salman Siddiqui, Fadi Al Machot

Faculty of Science and Technology (REALTEK)
Norwegian University of Life Sciences
NMBU
1430 Ås, Norway

ABSTRACT

In Generalized Zero-Shot Learning (GZSL), we aim to recognize both seen and unseen categories using a model trained only on seen categories. In computer vision, this translates into a classification problem, where knowledge from seen categories is transferred to unseen categories by exploiting the relationships between visual features and available semantic information, such as text corpora or manual annotations. However, learning this joint distribution is costly and requires one-to-one training with corresponding semantic information. We present a reversed conditional Diffusion-based model (RevCD) that mitigates this issue by generating semantic features synthesized from visual inputs by leveraging Diffusion models' conditional mechanisms. Our RevCD model consists of a cross Hadamard-Addition embedding of a sinusoidal time schedule and a multi-headed visual transformer for attention-guided embeddings. The proposed approach introduces three key innovations. First, we reverse the process of generating semantic space based on visual data, introducing a novel loss function that facilitates more efficient knowledge transfer. Second, we apply Diffusion models to zero-shot learning—a novel approach that exploits their strengths in capturing data complexity. Third, we demonstrate our model's performance through a comprehensive cross-dataset evaluation. The complete code will be available on GitHub.

Keywords Zero-Shot learning · Diffusion Model · Generative ZLS · Transfer Learning

1 Introduction

Zero-shot learning (ZSL) represents the state-of-the-art advancement in the domains of machine learning transferability and computer vision classification. By pushing the boundaries of knowledge extraction, we enable ML models to expand without costly retraining. This learning paradigm is particularly crucial as it addresses the inherent limitation of traditional machine learning models that require prior access to expensive datasets. ZSL leverages auxiliary knowledge, allowing models to explore unobserved events, edge cases, or new compositions without any additional training. Traditional approaches in ZSL focused on aligning attributes directly with object categories [26], while deep learning's potential to create a joint embedding space of visual and semantic features [8, 35, 7, 12, 41] have rendered this approach obsolete. The shift towards latent-based methods highlights the importance of embedding space techniques because of their ability to decode and infer complex data distributions. This offers a promising resolution to the two main challenges of ZSL, the semantic gap, and generalization abilities [44].

Our contribution introduces a Diffusion-based generative model, a notable innovation in ZSL. Distinct from conventional models that predominantly rely on attribute matching or embedding strategies, our RevCD model utilizes a diffusion process to model the data distributions iteratively, see Fig. 1. This augments the model's capability to manage class

*Corresponding author: William Heyden (e-mail: william.heyden@nmbu.no)

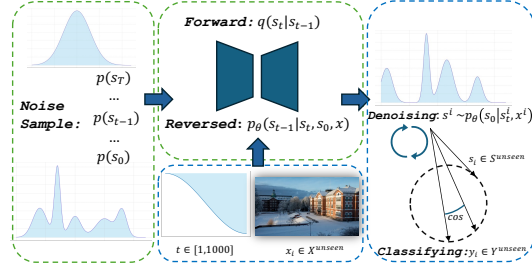


Figure 1: Overview of the proposed RevCD model: We train a denoising process using only seen samples (indicated by green boxes). Once trained, the model can estimate the semantic distribution by conditioning on the visual space of unseen samples (represented by blue boxes) and Gaussian noise. The final classification is conducted through a simple nearest-neighbor search based on the estimated density.

variability and enhances its generalization capacity. This control over the latent space is required for overcoming the challenges of bias and hubness commonly encountered in ZSL methodologies [27].

2 Related works

Advancements in likelihood-based models have been central to the progress of zero-shot learning [37]. By framing the learning process as a maximum likelihood estimation problem, these methods effectively model data distributions, allowing for robust generalization across both seen and unseen classes. This section categorizes ZSL approaches according to the foundational models employed for latent space approximation, including Variational Autoencoders (VAEs), Generative Adversarial Networks (GANs), and Hybrid models. Additionally, it highlights the role of attention mechanisms and embedding strategies in enhancing these models’ performance.

VAE-based. Variational Autoencoders [25] have played a crucial role in ZSL due to their probabilistic framework for modeling latent spaces. Their adaptability in synthesizing unseen class prototypes, as demonstrated by [39], [5], and [23], underscores their versatility in ZSL applications. For instance, [18] incorporates a semantic-guided approach within a VAE framework, while [46] employs a decoupling strategy to enhance performance. A significant advantage of VAEs lies in their capacity to *explicitly* approximate data density. However, a key limitation is their tendency to generate blurry or overly smoothed features due to posterior collapse [33], which can obscure essential class-specific details needed to distinguish between unseen classes.

GAN-based. Generative Adversarial Networks [14] offer a powerful and dynamic framework for feature synthesis. GANs have been successfully adapted to generate features for unseen classes; [13], [21], [15], and [53]. GANs ability to produce sharp and realistic features through *implicit* density estimation makes them particularly effective for capturing fine-grained details. However, they are also prone to challenges such as training instability and mode collapse [4], which can result in a lack of diversity in the generated features. This limitation may hinder the model’s ability to accurately represent the full spectrum of unseen classes.

Hybrids. Hybrid models in ZSL leverage multiple architectures to enhance performance. The majority of hybrid frameworks incorporate sequential modules, as seen in [16], [10] and [32]. Employing a VAE to learn an embedding function that constrains the semantic or visual space allows for greater control over the generation of synthesized features. Nevertheless, the complexity and computational overhead of combining multiple models can pose challenges, especially in terms of model interpretability and scalability.

Attention and embedding. Attention mechanisms [17, 24] and embedding strategies [1, 49] further refine the latent space by focusing on salient attributes and mapping visual data to semantic space. The approaches [48, 2, 31] enhance interpretability and feature distinctness; however, they rely heavily on high-quality, granular attribute information, which is not always available, limiting their applicability across diverse datasets.

Our contribution introduces a reversed Diffusion-based model (RevCD) for zero-shot inference. Diffusion models have been applied to improve accuracy as generative classifiers [6, 3, 40], and their capacity to generate synthetic data has been used to classify unseen compositions [9, 28]. However, these are limited by pre-training on prompt categories. Their implementation in a pure zero-shot setting is still absent. We address these limitations by leveraging the reversed process for generating conditioned semantic embeddings, aiming for effective generalization to unseen classes without the constraints observed in the aforementioned methodologies. **To the best of our knowledge, Diffusion models have not yet been explored in the ZSL domain.**

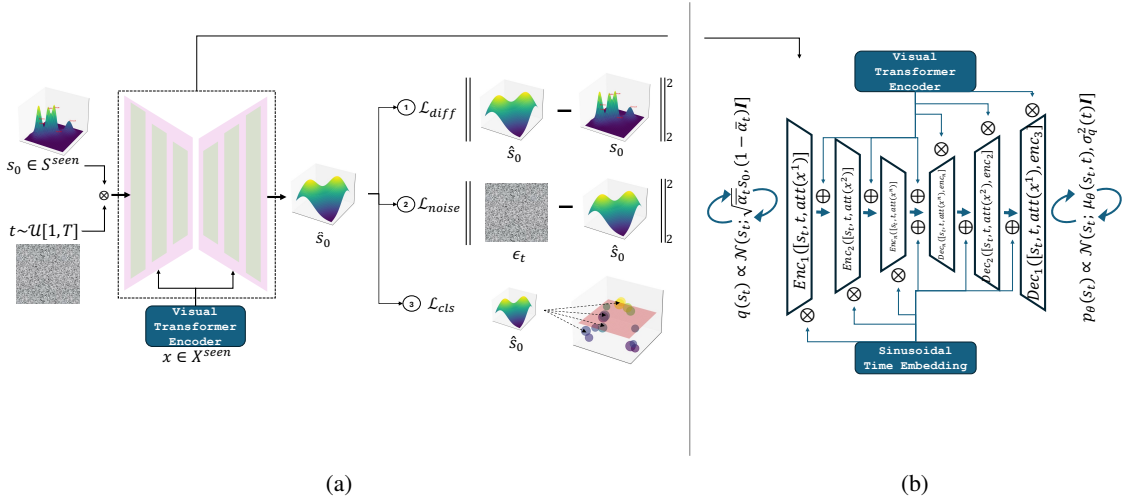


Figure 2: The figure illustrates our proposed approach for training. **(a)** presents our high-level architecture and associated loss functions. By conditioning the image, we can infer the semantic distribution of unseen classes. **(b)** provides a detailed view of our U-net architecture. It implements sinusoidal time and cross-Hadamard-Addition conditional embeddings for optimal control over the learned distribution. In ZSL, the goal is to transfer the knowledge of how to infer the distribution rather than the distribution itself.

3 Methodology

Problem Setup. We denote the set of seen images, semantics, and corresponding class labels as $\{x^{seen}, s^{seen}, y^{seen}\} \in \mathcal{D}^{seen}$, where x^{seen} represents the images, s^{seen} the semantics, and y^{seen} the class labels for the seen classes. The set of unseen semantics and class labels, denoted as $\{s^{unseen}, y^{unseen}\} \in \mathcal{D}^{unseen}$, represents the unseen dataset. During training, the model is trained exclusively on data from the seen set \mathcal{D}^{seen} , while assuming access to the semantic and label information of the unseen classes in \mathcal{D}^{unseen} . Importantly, the unseen images x^{unseen} are *not* available during training and are only introduced during the inference phase.

It is important to note that during training, the set of class labels for seen and unseen data do not overlap, i.e., $\mathcal{Y}^{seen} \cap \mathcal{Y}^{unseen} = \emptyset$.

During inference, the challenge is to map an unseen sample image, x^{unseen} , to its corresponding unseen label y^{unseen} , using a learned function $f: x^{unseen} \rightarrow y^{unseen}$.

The training process involves using paired examples $\{x^{seen}, s^{seen}\} \in \mathcal{D}^{seen}$ to learn a model, $p_\theta(s|x^{seen})$, that generalizes this mapping function from the visual features x^{seen} to their corresponding semantic features s^{seen} embedded in a shared semantic space. During the test phase, the semantic distribution of the unseen images x^{unseen} is approximated and subsequently classified into their corresponding unseen classes $y^{unseen} \in \mathcal{Y}^{unseen}$.

3.1 Diffusion Process

The diffusion process [42] models complex data distributions through a specific Markov chain structure. During training, we start with a clean semantic sample and its corresponding visual features $\{s_0, x\} \in \mathcal{D}^{seen}$. We incrementally infuse Gaussian noise using a fixed linear Gaussian model, which by using the reparameterization trick [25] can be parameterized by mean $\mu_t(s_t) = \sqrt{\alpha_t}s_{t-1}$, and variance $\Sigma(s_t) = (1 - \alpha)\mathbf{I}$ for hierarchical time-steps $t \in [0, T]$. Pre-defining a noise schedule $(\beta_1, \dots, \beta_T)$ allows us to sample from the Markov chain through a fixed forward sequence of time steps as:

$$q(s_t|s_{t-1}) = N(s_t; \sqrt{\alpha_t}s_{t-1}, (1 - \alpha_t)\mathbf{I}) \quad (1)$$

where $\alpha_t = 1 - \beta_t$ and $\bar{\alpha}_t = \prod_{i=1}^t \alpha_i$. This forward encoding process has the desired properties of being variance-preserving and completely deterministic, and the final distribution $p(s_T)$ is a standard Gaussian. Our aim is to learn a reverse process $p(s_{t-1}|s_t, x)$ which removes the noise of the forward process and can estimate a clean sample \hat{s}_0 from random noise conditioned on a visual space:

$$p(s_{0:T}|x) = p(s_T) \prod_{t=1}^T p(s_{t-1}|s_t, x) \quad (2)$$

Directly expressing p in closed form is intractable. We instead parameterize p_θ with θ and approximate the distribution by minimizing the evidence lower bound (ELBO) of the conditional log-likelihood

$$\log p_\theta(s|x) \geq \mathbb{E}_{q(s_{1:T}|s_0, x)} \left[\log \frac{p_\theta(s_0|s_{1:T}, x)p(s_{1:T}, x)}{q(s_{1:T}|s_0, x)} \right] \quad (3)$$

$$\begin{aligned} &= \underbrace{\mathbb{E}_{q(s_1, x|s_0)} [\log p_\theta(s_0|s_1, x)]}_{\text{reconstruction}} - \underbrace{D_{KL}[q(s_T|s_0, x)||p(s_T|x)]}_{\text{prior matching}} \\ &\quad - \underbrace{\sum_{t=2}^T \mathbb{E}_{q(s_t, x|s_0)} [D_{KL}[q(s_{t-1}|s_t, s_0, x)||p_\theta(s_{t-1}|s_t, x)]]}_{\text{diffusion term}} \end{aligned} \quad (4)$$

By conditioning the forward process on the clean example at any given t , the diffusion loss can be formulated using Bayes rule as the KL divergence between the analytical truth denoising step $q(s_{t-1}|s_t, s_0, \mathbf{x})$ and our approximated denoising step $p_\theta(s_{t-1}|s_t, \mathbf{x})$. The prior loss $D_{KL}[q(s_T|s_0, x)||p(s_T|x)]$ can be ignored as it does not contain any trainable parameters and is zero under our assumption. The reconstruction loss $\log p_\theta(s_0|s_1, x)$ is typically minimal and can be safely ignored without affecting the outcome. Therefore, our diffusion objective becomes:

$$\arg \max_{\theta} \mathbb{E}_{t \sim [2, T]} [\mathbb{E}_q [D_{KL}(q(s_{t-1}|s_t, s_0) || p_\theta(s_{t-1}|s_t, x))]] \quad (5)$$

which boils down to learning a neural network, s_θ , to predict the semantic space \hat{s}_0 from noise at time t , conditioned on an image x . This network can be optimized using stochastic samples of t from a uniform distribution $t \sim \mathcal{U}[0, T]$. Given our case, where we can set the variances to match exactly, the KL divergence in Eq. (5) can be reduced to a minimization of the difference between the mean of the two distributions [11]. We arrive to our diffusion loss (loss ① in Fig. 2a):

$$\mathcal{L}_{Diffusion} = \underbrace{\frac{1}{2\sigma_q^2(t)} \frac{\bar{\alpha}_{t-1}(1-\alpha_t)^2}{(1-\bar{\alpha}_t)^2}}_{w_t} [||\hat{s}_\theta(s_t, t, \mathbf{x}) - s_0||_2^2] \quad (6)$$

The first term is a time-dependent variance weight, where $\sigma_q^t(t) = \beta_t$ [19]. However, empirical research [28] has demonstrated that setting $w_t = 1$ yields optimal performance and our results from a zero-shot paradigm show similar results.

3.1.1 Cross Hadamard-Addition Embeddings

In the traditional diffusion process, we predict the ground truth of a noisy sample at time t . In our approach, however, we further condition this process on visual features. Consequently, the neural network s_θ is trained on the triplet (s_t, t, x) , where $\{s, x\} \in \mathcal{D}^{seen}$. To refine the embeddings for both the conditioning variable x and the time-step schedule t , we employ a cross Hadamard-Addition method, which enhances the representation and integration of these features within the network. During the representational mapping stage within the network, we use Hadamard integration for the time-step input, acknowledging that the added noise is entirely deterministic, while integrating the visual condition through addition (refer to the encoding step in Fig. 2b). In contrast, during the network’s generative stage, we reverse these roles, applying Hadamard integration for a stronger conditional reconstruction and a more relaxed incorporation of the time-step input (see the decoding step in Fig. 2b). We observed that this approach resulted in a closer alignment of the joint probability space with the reconstructed features, leading to improved accuracy.

Time-dependent embedding. To increase the dimension of the time step, t , we employ a sinusoidal time embedding $\bar{t} \leftarrow TE(t, d)$:

$$TE(t, d) = [\cos(t \cdot f_0), \sin(t \cdot f_0), \dots, \cos(t \cdot f_{\frac{d}{2}-1}), \sin(t \cdot f_{\frac{d}{2}-1})] \quad (7)$$

where d is the embedding dimension and f_i are frequencies. The temporal encoding dimension is matched layer-wise with the network to better learn a denoising function. This is crucial for accurately reconstructing $s \in S_{\text{seen}}$ and preparing for generalization to S_{unseen} .

Visual-dependent embedding. We implement a Transformer encoder [43] to extract visual features for conditioning. These visual features are integrated into the network at each layer, with the Transformer trained concurrently. To align the denoising feature dimensions, we map the multi-head attention outputs from the visual space to each intermediate feature using a Hadamard product in the decoder and matrix addition in the encoder of our denoising model (see Fig. 2b).

3.2 Noise Loss

The diffusion loss in Eq. (4) can also be interpreted as estimating the source noise $\hat{\epsilon}_t$, rather than directly predicting the clean sample \hat{s}_0 . By applying the reparameterization trick [34], we can express the relationship between a clean and an arbitrarily noised sample as:

$$s_0 = \frac{s_t - \sqrt{1 - \bar{\alpha}_t} \epsilon_0}{\sqrt{\bar{\alpha}_t}} \quad (8)$$

This enables us to estimate the reverse transition mean by directly utilizing the estimated added noise instead:

$$\mu_\theta(s_t, t) = \frac{1}{\sqrt{\alpha_t}} s_t - \frac{1 - \alpha_t}{\sqrt{1 - \bar{\alpha}_t} \sqrt{\alpha_t}} \hat{\epsilon}_t \quad (9)$$

This approach allows us to optimize the KL divergence in Eq. (5) as a function of the perturbed noise at time step t . In our diffusion setting, where the variance of the forward and reverse processes aligns, the KL divergence between the ground truth and the approximated denoising step (via the U-Net) can be optimized by estimating the source noise from the predicted noise. Leveraging this theoretical perspective, we introduce an additional noise loss term that corresponds to our clean-sample predictor (loss ② in Fig. 2a):

$$\mathcal{L}_{noise} = \frac{1}{2\sigma_q^2(t)} \underbrace{\frac{(1 - \alpha_t)^2}{(1 - \bar{\alpha}_t)^2 \alpha_t}}_{w'_t} \|\epsilon_0 - (\hat{s}_\theta(s_t, t, x) - s_0)\|_2^2 \quad (10)$$

Note the slight variance-weighting difference compared to the diffusion loss in Eq. (6). This discrepancy is a correction term as a result of the different transition mean calculation. However, it can be eliminated by assigning a fixed constant value of $w'_t = 1$.

These two complementary formulations of the denoising transition mean correspond to an equivalent optimization problem (Eq. 5). While they introduce additional complexity to the optimization process, necessitating more sophisticated strategies and careful hyperparameter tuning to achieve convergence, we observe significant improvements in feature generation. We believe that this loss function acts as a regularizer during optimization, enhancing the model’s ability to generalize to unseen data. By optimizing from multiple perspectives, the model generates richer and more robust representations.

3.3 Classification loss

Unlike other generative models, like flow-based models and GANs, Diffusion models have no natural property to decrease the intra-class variance from the noise input [20]. Previous work in classifier- and classifier-free guidance in score-based Diffusion models [20] involves modifying the score function with the gradient of the log-likelihood of a separate classifier model $-\eta \nabla_\vartheta \log p_\vartheta(y|s_t)$. Our classification objective is to steer our optimization problem of the inferred distribution through manifold regularization [47], leveraging a classifier

$$\arg \max_{\theta} \mathbb{E}_{y \in Y_{\text{seen}}} [\log p_\theta(\hat{s}_{0:T}|y)] \quad (11)$$

This allows us to approximate samples from the distribution $p_\theta(y|s_t) \propto p_\theta(s_t|y)p_\theta(y)$. This strategy of assigning higher likelihood to the correct label has led to notable improvements in both the perceptual qualities and the inception scores of models, as highlighted in prior research [38]. However, within the zero-shot learning framework, our goal

Algorithm 1 Training algorithm for RevCD**Ensure:**

$$\bar{t} \sim TE(\mathcal{U}[0, 1], d)$$

$$\epsilon \sim \mathcal{N}(0, \mathbf{I})$$

for $s_0, \mathbf{x} \sim p(x, s) \in \mathcal{D}^{seen}$ **do**

$$\hat{s}_0 \leftarrow \|\text{Unet}(\sqrt{\bar{\alpha}_t}s_0 + \sqrt{(1-\bar{\alpha}_t)}\epsilon, \bar{t}, x) - \sqrt{\bar{\alpha}_t}s_0 + \sqrt{(1-\bar{\alpha}_t)}\epsilon\|_2^2$$

$$\hat{y} \leftarrow \mathbb{E}_\vartheta(\hat{s}_0 | y_{seen})$$

$$\hat{\epsilon}_t \leftarrow \|\epsilon_0 - (\hat{s}_0 - \epsilon_t)\|_2^2$$

end for

Gradient step on:

$$\nabla_\theta [(1-\lambda)\mathcal{L}_{Diff}(\hat{s}_0) + \lambda\mathcal{L}_{cls}(\hat{y}) + \eta\mathcal{L}_{noise}(\hat{\epsilon}_t)]$$

shifts towards enhancing the model’s ability to generalize the learned distribution for generating samples. These samples are not primarily focused on visual appeal but are aimed at positioning the probability mass of each conditional sample at a greater distance, leading to enhanced recognition of unseen classes. We hence formulate the loss as the expectation over the empirical sample distribution $\mathbb{E}[\mathcal{L}(f(\mathbf{x}; \vartheta), y_x)]$ and implement this with a cross-entropy loss (loss ③ in Fig. 2a):

$$\mathcal{L}_{cls} = -\frac{1}{n} \sum_{i=1}^n \sum_{j=1}^c y_{ij} \log p_\vartheta(\hat{y}_{ij} | s_i) \quad (12)$$

where n is the number of samples, y_{ij} and \hat{y}_{ij} is the true and predicted label of for class j of the i -th instance.

3.4 Model Architecture

Our denoising Diffusion model employs a U-net architecture, as introduced by the probabilistic diffusion model in [19]. To merge visual and semantic information effectively, we have customized this architecture to support both our time-dependent and visual-dependent embeddings, as illustrated in Fig 2b. To our knowledge, this represents the first application of a U-net architecture tailored for zero-shot learning in such a specific way. The encoder-decoder structure of our U-net is built from linear blocks featuring ReLU non-linearity and batch normalization. Inputs to each layer include sinusoidal time embeddings and conditional data, which are extracted using self-attention mechanisms and augmented by a skip-connection between the encoding and decoding stages.

3.5 Training Objective

Our main idea focuses on directly modeling the semantic posterior using variational inference rooted in Eq. (13). We achieve this by disentangling the posterior estimation into three key components: noise prediction, data reconstruction, and classification. This decomposition results in a more complex and nuanced loss landscape [29]. Despite the increased complexity, integrating these distinct loss components enhances the model’s generalization capabilities. This is primarily due to the regularization effects inherent in the multi-faceted loss function and the fine-tuning achieved through careful hyperparameter optimization.

$$\mathcal{L}_{total} = (1-\lambda)\mathcal{L}_{diffusion} + \lambda\mathcal{L}_{classification} + \eta\mathcal{L}_{noise} \quad (13)$$

Here, λ serves as a balancing factor between the objectives of reconstruction and classification, while the hyperparameter η acts as a regularization coefficient. Through this, the probability distribution of the samples aligns with the expectation of the generated conditional samples $p(s) \propto \mathbb{E}_{x \sim p(x)}[p_\theta(s|x)]$. The implementation details of this loss function during training are provided in Algorithm (1).

3.6 Sampling

Using standard methods from diffusion theory [19], we generate the semantic embedding space of an unseen sample through iterative conditional denoising using our trained model, as shown in Algorithm (2). Samples are drawn from the standard normal prior $p(s_T) \sim \mathcal{N}(0, \mathbf{I})$ and denoised conditioned on the sinusoidal time-step embedding $\bar{t}_i \forall i \in [1000, 0]$ and the Transformer-encoded latent visual space $x \in \mathcal{D}^{unseen}$.

Algorithm 2 Unseen sampling algorithm for RevCD**Ensure:**

```

 $s_t \sim \mathcal{N}(0, \mathbf{I})$ 
 $x \sim p(x|y) \in \mathcal{D}^{unseen}$ 
for  $t = T, \dots, 1$  do
   $\bar{t} \leftarrow TE(t, d)$ 
   $\hat{s}_t \leftarrow U_{net}(s_t, x \oplus s, \bar{t})$ 
   $s_{t-1} \leftarrow \frac{1}{\sqrt{\alpha_t}}(s_t - \frac{(1-\alpha_t)\hat{s}_t}{\sqrt{1-\alpha_t}}) + \beta_t z$ 
end for
return  $\hat{s}_0$ 

```

The sampling through the reversed diffusion process is crucial for synthesizing high-quality semantic embeddings from the noised data. This process is governed by the following equation:

$$s_{t-1} = \underbrace{\frac{1}{\sqrt{\alpha_t}}(s_t - \frac{(1-\alpha_t)\hat{s}_t}{\sqrt{1-\alpha_t}})}_{\text{remove noise}} + \underbrace{\beta_t z}_{\text{add noise}} \quad (14)$$

Here, s_{t-1} denotes the noisy semantic embeddings at time step $t - 1$, \hat{s}_t represents the (predicted) noised sample at previous time step t , and β_t is the variance noise vector that controls the amount of noise added back to ensure stability, where $z \sim \mathcal{N}(0, I)$. This iterative refinement process enables the model to generate \hat{s}^{unseen} during inference.

3.7 Zero-Shot Inference

In the zero-shot learning setting, the model utilizes the approximated semantic embeddings \hat{s}^{unseen} to classify instances of unseen classes using a nearest-neighbor approach in the semantic space. Leveraging the semantic embeddings to bridge the gap between visual features of x^{unseen} and class labels y^{unseen} :

$$\hat{y} = \arg \min_{y \in \mathcal{Y}^{unseen}} \text{distance}(\hat{s}^{unseen}, s_y^{unseen}), \quad (15)$$

where \hat{y} is the predicted class label for an unseen class instance, and $\text{distance}(\cdot, \cdot)$ is a distance metric, in our case cosine similarity:

$$\text{dist}(i, j) = 1 - \frac{\langle s_i, s_j \rangle}{\|s_i\|_2 \|s_j\|_2} \quad (16)$$

4 Experimental results

We evaluate our approach by measuring classification accuracy on both known and unknown categories. Importantly, samples from unknown categories are entirely absent during training, ensuring that classification accuracy for these categories reflects the model’s ability to transfer knowledge from the known space. This evaluation methodology aligns with established practices in zero-shot inference research, facilitating fair comparison and assessment of our model’s performance.

Dataset. Our analysis of diffusion as a generative method for zero-shot inference employs four publicly available benchmark datasets, distinct within the field. This allows us to make a fair comparison of the quality and coverage approximated semantics. The datasets are: Scene Understanding Attribute dataset (SUN) [36], Caltech Birds dataset (CUB200-2011) [45], Animals with Attributes 2 dataset (AwA2) [52], and Attribute Pascal and Yahoo dataset (APY).

The CUB dataset, focused on bird species, offers detailed representations in both image and semantic spaces. In contrast, AWA, which covers animal species, provides coarser descriptions in both domains. SUN, a scenery dataset, spans a wide range of classes, while APY consists of general objects with a limited, broad semantic description.

Visual features are derived using a ResNet101 backbone pre-trained on ImageNet [50]. We only compare models using similar image features to ensure equitable. The semantic attributes released with the respective datasets are implemented, consisting of crowd-sourced human studies or word2vector label extractions.

Implementation details. The employed U-net architecture for our Diffusion model consists of three hidden, fully connected dense layers, ReLU activation function, and dropout for regularization. We use a feature extractor with

Table 1: Result of generalized ZSL for classification, for the most prominent generative approaches. † denotes the model consists of additional components that are disregarded.

Generative model	Name	AwA			CUB			SUN			aPY		
		Seen	Unseen	Harm.	Seen	Unseen	Harm.	Seen	Unseen	Harm.	Seen	Unseen	Harm.
VAE†	cVAE [7]	72.6	54.4	62.2	59.9	47.0	52.7	-	-	-	55.3	30.2	39.0
GAN†	GAN [13]	82.4	24.7	38.1	44.4	31.3	36.8	43.3	29.0	31.4	50.0	25.1	33.4
Diffusion (ours)	RevCD	82.4	49.2	63.8	57.4	40.2	47.3	58.2	51.2	54.4	63.6	36.7	46.5

a multi-head self-attention layer (MSA) for the conditional space. In the encoder and the decoder of the U-net, we concatenate and add the sinusoidal time embedding to layer inputs and the conditional features as explained in section 3.1.1.

4.1 Generalized accuracy

We demonstrate semantic posterior sampling using our Diffusion model. To evaluate its performance, we consider two natural comparisons. (I) Models that use variational inference to approximate the posterior, such as VAEs, which are optimized by balancing reconstruction accuracy and the divergence between the approximate and true posterior distributions; and (II) models that use indirect approaches to approximate the distribution, such as GANs, which achieve posterior matching through adversarial training.

These comparisons are summarized in Table 1. As shown, no single generative model consistently outperforms the others across all datasets when generating both seen and unseen samples. Notably, our method surpasses the other approaches in generating samples on three of the four datasets when measured by the harmonic mean. The most significant performance gap is observed in the semantically coarse SUN dataset, where our approach achieves a 20% improvement over GANs. A similar trend is evident in the class-diverse APY and AWA datasets, albeit with smaller margins. In contrast, the CUB dataset, which features a wide variety of fine-grained semantic details, proves challenging for denoising approaches, making variational inference methods a more effective fit.

VAEs benefit from the tractable estimation of the posterior distribution, as evidenced by a 5.4% higher harmonic mean when both seen and unseen samples are drawn from tighter distributions, such as those observed in the CUB dataset, which emphasizes local descriptions. In contrast, GANs appear to struggle in this context, likely due to mode collapse in the posterior. Our Diffusion model performs moderately, achieving a 10.4% improvement over GANs.

Conversely, GANs implicitly learn the distribution through adversarial training, which encourages the generator to produce high-fidelity samples, as demonstrated in the AWA dataset, where attributes emphasize global image descriptions. However, the absence of explicit density estimation makes GANs susceptible to seen-unseen bias, leading to a preference for the seen distribution during inference, as observed in both the SUN and APY datasets. Our Diffusion model shows strong performance in generating samples when the seen distribution is discriminative and low-dimensional, as in the AWA and APY datasets. However, it struggles to maintain a tight lower bound on the true

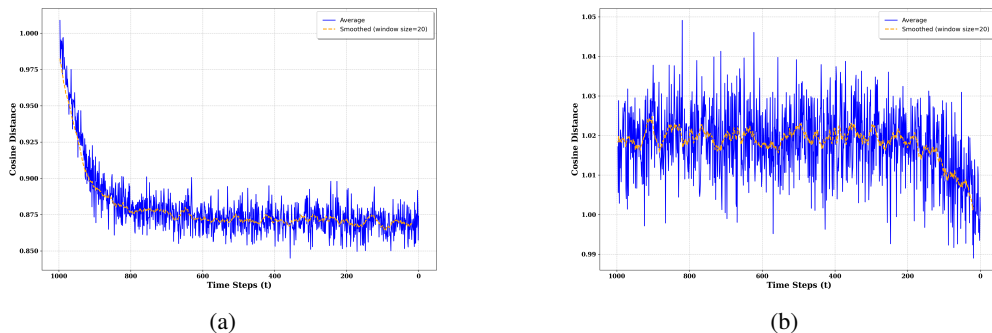


Figure 3: The cosine distance to the true semantic space and the denoised learned representation are shown for both the AWA dataset and the CUB dataset. (a) For AWA, we observed a rapid reduction in noise in the initial timesteps, which gradually slowed as it approached the fully denoised space. (b) Conversely, for the CUB dataset, which possesses a semantically fine-grained space, the reduction in noise exhibited an inverse pattern.

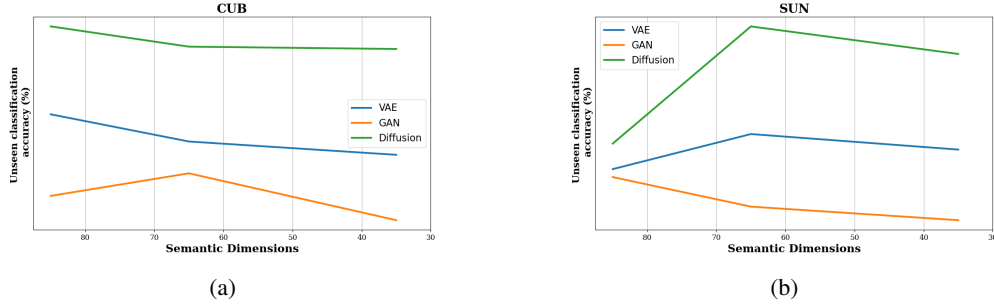


Figure 4: We measure the effectiveness in terms of accuracy of unseen classification through nearest neighbour search of pure generative models VAE, GAN, and Diffusion. The semantic dimension is decreasing through filtering of principal components used to generate novel samples.

data distribution as the dimensionality of the semantic space increases, as evidenced by its performance in the CUB dataset.

This pattern is evident in Fig. 3, which illustrates the sample quality during iterative denoising. In Fig. 3(a), the density of seen samples in the AWA dataset is reproduced more quickly compared to the higher-dimensional space in the CUB dataset, as shown in Fig. 3(b).

Table 2 compares our Diffusion model with top-performing established zero-shot classification approaches. For SUN, our Diffusion model outperforms other approaches in the generation of the seen sample by a margin of 21.6%, with only a minor deficiency in unseen generation of 1.1% compared to f-CLSWGAN [51] and DAZLE [22] respectively. For CUB and APY, our model performs comparably to the other models. The pattern of the results indicates that generative models effectively outperform embedding-based approaches, with our Diffusion model being no exception.

Table 2: Comparative table for previously established methods in the field. The reported results are the generalized zero-shot per-class average results for seen (S), unseen (U) and harmonic mean (H) as reported in the respective papers.

Methods	AWA2			CUB			SUN			APY		
	S	U	H	S	U	H	S	U	H	S	U	H
<i>Embedding approach</i>												
ALE [1]	81.8	14.0	23.9	62.8	23.7	34.4	33.1	21.8	26.3	-	-	-
LATEM [49]	77.3	11.5	20.0	57.3	15.2	24.0	28.8	14.7	19.5	-	-	-
PQZSL [30]	-	-	-	43.2	51.4	46.9	35.1	35.3	35.2	64.1	27.9	38.8
<i>Generative approach</i>												
f-CLSWGAN [51]	68.9	52.1	59.4	57.7	43.7	49.7	36.6	42.6	39.4	61.7	32.9	42.9
CADA-VAE [39]	75.0	55.8	63.9	53.5	51.6	52.5	35.7	47.2	40.6	-	-	-
DAZLE [22]	75.7	60.3	67.1	59.6	56.7	58.1	24.3	52.3	33.2	-	-	-
RevCD (Ours)	82.4	49.2	63.8	57.4	40.2	47.3	58.2	51.2	54.4	63.6	36.7	43.1

Toy experiment: The effect of a lower dimension space. We explore how the implicit density modeling framework of our Diffusion model captures the distribution of the semantic space in a reduced setting. This ability allows our model to be implemented in environment where capturing broad auxiliary information is costly or infeasible. Fig. 4 exemplifies this by reducing the dimensions of the semantic space by capturing the principal components of the respective datasets and comparing them to the generative capabilities of a conditional VAE and a conditional GAN. We observe that our Diffusion model maintains solid performance in the generative estimation of unseen classes when only condensed information is available. Only a 2% decrease can be seen as we reduce the dimensions in CUB and 15% in SUN. We hypothesise that the cross Hadamard-Addition embedding captures available information during iterative denoising. This reduces the dependence on a single condition at any given time and allows the generative process to gradually be guided in the right direction.

The VAEs conditioned on the same semantic representation exhibit a decline of 8% in density estimation for unseen classes in CUB as the dimensionality is reduced. The GAN also suffers from a notable decline in SUN with a 10% decline.

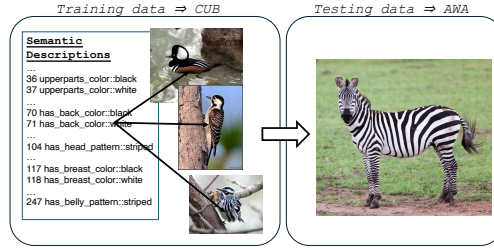


Figure 5: Conceptual understanding of cross-examining datasets. The semantic description of black and white stripes found on bird species is transferred from the bird dataset CUB to the animal dataset AWA.

Comparative analysis of performance across various domains. As for humans, classifying different species of birds requires finer scaled knowledge than classifying different species of animals. By cross-examining the datasets, we show that our approach not only reduced the training impact within a domain but actually can be reused across granularity, further reducing the overall training required. Our experiments show that our model is able to capture a few labels well in different datasets while missing other labels. We found that classes with semantic overlaps can be transferred across datasets, see Fig. (5). However, where the overlap is of no semantic similarity, i.e., sceneries in SUN, the performance is significantly reduced. Table 3 reports the average accuracy across *unseen* classes. We see that the model also performs better when the dimensional space of the test dataset is smaller, i.e. for APY. We recognise that performance is significantly reduced but argue the model is still utilizing learned knowledge where applicable.

To the best of our knowledge, there has been limited cross-examination of datasets in ZSL research, providing little foundation for direct comparison. We argue that training across different source domains offers valuable insights and suggest that future work should explore the characteristics of classes that are more easily transferable.

Table 3: Average accuracy for unseen classification in the datasets. Blue shading denotes that the model was trained in a reduced-dimensional space to accommodate the testing data, while green shading indicates that the model was trained in the original dimensional space but tested on a reduced-dimensional dataset to align with the trained model.

%	Trained on			
	CUB	SUN	AWA	APY
Tested on				
CUB	-	1.6	15.1	7.9
SUN	1.3	-	7.8	1.0
AWA	11.1	3.9	-	1.5
APY	8.0	7.9	10.2	-

5 Conclusion

In this paper, we introduce a reversed Conditional Diffusion model (RevCD) and evaluate its performance against VAEs and GANs for zero-shot learning. This foundational research explores the largely untapped potential of diffusion-based models to generate unseen samples. Our RevCD model generates samples for classes that serve as prototypes for high-accuracy classification. By leveraging visual conditioning, our approach allows precise control over the generation process, outperforming other generative methods in settings with unseen classes. Experimental results demonstrate the advantages of using a diffusion model as a generative backbone, especially regarding its robustness to limited semantic information. We believe our findings can stimulate further exploration of diffusion models in generalized zero-shot learning (GZSL). Moreover, expanding cross-dataset evaluations in future zero-shot learning research could lead to the development of more resilient models.

References

- [1] Z. Akata, F. Perronin, Z. Harchaoui, and C. Schmid. Label-embedding for image classification. *IEEE transactions on pattern analysis and machine intelligence*, 38(7):1425–1438, 2015.
- [2] F. Alamri and A. Dutta. Implicit and explicit attention mechanisms for zero-shot learning. *Neurocomputing*, 534:55–66, 2023.
- [3] S. Azizi, S. Kornblith, C. Saharia, M. Norouzi, and D. J. Fleet. Synthetic data from diffusion models improves imagenet classification. *arXiv preprint arXiv:2304.08466*, 2023.
- [4] D. Bau, J.-Y. Zhu, J. Wulff, W. Peebles, H. Strobel, B. Zhou, and A. Torralba. Seeing what a gan cannot generate. In *Proceedings of the IEEE/CVF international conference on computer vision*, pages 4502–4511, 2019.
- [5] M. Bucher, S. Herbin, and F. Jurie. Generating visual representations for zero-shot classification. In *Proceedings of the IEEE International Conference on Computer Vision Workshops*, pages 2666–2673, 2017.
- [6] H. Chen, Y. Dong, Z. Wang, X. Yang, C. Duan, H. Su, and J. Zhu. Robust classification via a single diffusion model. *arXiv preprint arXiv:2305.15241*, 2023.
- [7] Z. Chen, Y. Luo, R. Qiu, S. Wang, Z. Huang, J. Li, and Z. Zhang. Semantics disentangling for generalized zero-shot learning. In *Proceedings of the IEEE/CVF international conference on computer vision*, pages 8712–8720, 2021.
- [8] Z. Chen, S. Wang, J. Li, and Z. Huang. Rethinking generative zero-shot learning: An ensemble learning perspective for recognising visual patches. In *Proceedings of the 28th ACM International Conference on Multimedia*, pages 3413–3421, 2020.
- [9] K. Clark and P. Jaini. Text-to-image diffusion models are zero shot classifiers. *Advances in Neural Information Processing Systems*, 36, 2024.
- [10] B. Ding, Y. Fan, Y. He, and J. Zhao. Enhanced vaegan: a zero-shot image classification method. *Applied Intelligence*, 53(8):9235–9246, 2023.
- [11] J. Duchi. Derivations for linear algebra and optimization. *Berkeley, California*, 3(1):2325–5870, 2007.
- [12] A. Frome, G. S. Corrado, J. Shlens, S. Bengio, J. Dean, M. Ranzato, and T. Mikolov. Devise: A deep visual-semantic embedding model. *Advances in neural information processing systems*, 26, 2013.
- [13] R. Gao, X. Hou, J. Qin, J. Chen, L. Liu, F. Zhu, Z. Zhang, and L. Shao. Zero-vae-gan: Generating unseen features for generalized and transductive zero-shot learning. *IEEE Transactions on Image Processing*, 29:3665–3680, 2020.
- [14] I. Goodfellow, J. Pouget-Abadie, M. Mirza, B. Xu, D. Warde-Farley, S. Ozair, A. Courville, and Y. Bengio. Generative adversarial nets. *Advances in neural information processing systems*, 27, 2014.
- [15] A. Gupta, S. Narayan, S. Khan, F. S. Khan, L. Shao, and J. van de Weijer. Generative multi-label zero-shot learning. *IEEE Transactions on Pattern Analysis and Machine Intelligence*, 2023.
- [16] Z. Han, Z. Fu, S. Chen, and J. Yang. Contrastive embedding for generalized zero-shot learning. In *Proceedings of the IEEE/CVF conference on computer vision and pattern recognition*, pages 2371–2381, 2021.
- [17] S. Hao, K. Han, and K.-Y. K. Wong. Learning attention as disentangler for compositional zero-shot learning. In *Proceedings of the IEEE/CVF Conference on Computer Vision and Pattern Recognition*, pages 15315–15324, 2023.
- [18] W. Heyden, H. Ullah, M. S. Siddiqui, and F. Al Machot. An integral projection-based semantic autoencoder for zero-shot learning. *IEEE Access*, 2023.
- [19] J. Ho, A. Jain, and P. Abbeel. Denoising diffusion probabilistic models. *Advances in neural information processing systems*, 33:6840–6851, 2020.
- [20] J. Ho and T. Salimans. Classifier-free diffusion guidance. *arXiv preprint arXiv:2207.12598*, 2022.
- [21] H. Huang, C. Wang, P. S. Yu, and C.-D. Wang. Generative dual adversarial network for generalized zero-shot learning. In *Proceedings of the IEEE/CVF conference on computer vision and pattern recognition*, pages 801–810, 2019.
- [22] D. Huynh and E. Elhamifar. Fine-grained generalized zero-shot learning via dense attribute-based attention. In *Proceedings of the IEEE/CVF conference on computer vision and pattern recognition*, pages 4483–4493, 2020.
- [23] Z. Ji, B. Cui, Y. Yu, Y. Pang, and Z. Zhang. Zero-shot classification with unseen prototype learning. *Neural computing and applications*, pages 1–11, 2023.

- [24] M. G. Z. A. Khan, M. F. Naeem, L. Van Gool, A. Pagani, D. Stricker, and M. Z. Afzal. Learning attention propagation for compositional zero-shot learning. In *Proceedings of the IEEE/CVF Winter Conference on Applications of Computer Vision*, pages 3828–3837, 2023.
- [25] D. P. Kingma and M. Welling. Auto-encoding variational bayes. *arXiv preprint arXiv:1312.6114*, 2013.
- [26] C. H. Lampert, H. Nickisch, and S. Harmeling. Learning to detect unseen object classes by between-class attribute transfer. In *2009 IEEE conference on computer vision and pattern recognition*, pages 951–958. IEEE, 2009.
- [27] A. Lazaridou, G. Dinu, and M. Baroni. Hubness and pollution: Delving into cross-space mapping for zero-shot learning. In *Zong C, Strube M, editors. Proceedings of the 53rd Annual Meeting of the Association for Computational Linguistics and the 7th International Joint Conference on Natural Language Processing (Volume 1: Long Papers); 2015 Jul 26-31; Beijing, China. Stroudsburg (PA): Association for Computational Linguistics; 2015. p. 270-80.* ACL (Association for Computational Linguistics), 2015.
- [28] A. C. Li, M. Prabhudesai, S. Duggal, E. Brown, and D. Pathak. Your diffusion model is secretly a zero-shot classifier. In *Proceedings of the IEEE/CVF International Conference on Computer Vision*, pages 2206–2217, 2023.
- [29] H. Li, Z. Xu, G. Taylor, C. Studer, and T. Goldstein. Visualizing the loss landscape of neural nets. *Advances in neural information processing systems*, 31, 2018.
- [30] J. Li, X. Lan, Y. Liu, L. Wang, and N. Zheng. Compressing unknown images with product quantizer for efficient zero-shot classification. In *Proceedings of the IEEE/CVF Conference on Computer Vision and Pattern Recognition*, pages 5463–5472, 2019.
- [31] Y. Li, Z. Liu, S. Jha, and L. Yao. Distilled reverse attention network for open-world compositional zero-shot learning. In *Proceedings of the IEEE/CVF International Conference on Computer Vision*, pages 1782–1791, 2023.
- [32] Y. Liu, K. Tao, T. Tian, X. Gao, J. Han, and L. Shao. Transductive zero-shot learning with generative model-driven structure alignment. *Pattern Recognition*, page 110561, 2024.
- [33] J. Lucas, G. Tucker, R. B. Grosse, and M. Norouzi. Don’t blame the elbo! a linear vae perspective on posterior collapse. *Advances in Neural Information Processing Systems*, 32, 2019.
- [34] C. Luo. Understanding diffusion models: A unified perspective. *arXiv preprint arXiv:2208.11970*, 2022.
- [35] A. Mishra, S. Krishna Reddy, A. Mittal, and H. A. Murthy. A generative model for zero shot learning using conditional variational autoencoders. In *Proceedings of the IEEE conference on computer vision and pattern recognition workshops*, pages 2188–2196, 2018.
- [36] G. Patterson and J. Hays. Sun attribute database: Discovering, annotating, and recognizing scene attributes. In *2012 IEEE Conference on Computer Vision and Pattern Recognition*, pages 2751–2758. IEEE, 2012.
- [37] F. Pourpanah, M. Abdar, Y. Luo, X. Zhou, R. Wang, C. P. Lim, X.-Z. Wang, and Q. J. Wu. A review of generalized zero-shot learning methods. *IEEE transactions on pattern analysis and machine intelligence*, 45(4):4051–4070, 2022.
- [38] T. Salimans, I. Goodfellow, W. Zaremba, V. Cheung, A. Radford, and X. Chen. Improved techniques for training gans. *Advances in neural information processing systems*, 29, 2016.
- [39] E. Schonfeld, S. Ebrahimi, S. Sinha, T. Darrell, and Z. Akata. Generalized zero-and few-shot learning via aligned variational autoencoders. In *Proceedings of the IEEE/CVF conference on computer vision and pattern recognition*, pages 8247–8255, 2019.
- [40] J. Shipard, A. Wiliem, K. N. Thanh, W. Xiang, and C. Fookes. Diversity is definitely needed: Improving model-agnostic zero-shot classification via stable diffusion. In *Proceedings of the IEEE/CVF Conference on Computer Vision and Pattern Recognition*, pages 769–778, 2023.
- [41] R. Socher, M. Ganjoo, C. D. Manning, and A. Ng. Zero-shot learning through cross-modal transfer. *Advances in neural information processing systems*, 26, 2013.
- [42] J. Sohl-Dickstein, E. Weiss, N. Maheswaranathan, and S. Ganguli. Deep unsupervised learning using nonequilibrium thermodynamics. In *International conference on machine learning*, pages 2256–2265. PMLR, 2015.
- [43] A. Vaswani, N. Shazeer, N. Parmar, J. Uszkoreit, L. Jones, A. N. Gomez, Ł. Kaiser, and I. Polosukhin. Attention is all you need. *Advances in neural information processing systems*, 30, 2017.
- [44] V. K. Verma and P. Rai. A simple exponential family framework for zero-shot learning. In *Machine Learning and Knowledge Discovery in Databases: European Conference, ECML PKDD 2017, Skopje, Macedonia, September 18–22, 2017, Proceedings, Part II 10*, pages 792–808. Springer, 2017.
- [45] C. Wah, S. Branson, P. Welinder, P. Perona, and S. Belongie. The caltech-ucsd birds-200-2011 dataset. ", 2011.

-
- [46] Q. Wang and T. P. Breckon. Generalized zero-shot domain adaptation via coupled conditional variational autoencoders. *Neural Networks*, 163:40–52, 2023.
 - [47] Y. Wang, S. Chen, H. Xue, and Z. Fu. Semi-supervised classification learning by discrimination-aware manifold regularization. *Neurocomputing*, 147:299–306, 2015.
 - [48] Y. Wang, L. Feng, X. Song, D. Xu, and Y. Zhai. Zero-shot image classification method based on attention mechanism and semantic information fusion. *Sensors*, 23(4):2311, 2023.
 - [49] Y. Xian, Z. Akata, G. Sharma, Q. Nguyen, M. Hein, and B. Schiele. Latent embeddings for zero-shot classification. In *Proceedings of the IEEE conference on computer vision and pattern recognition*, pages 69–77, 2016.
 - [50] Y. Xian, C. H. Lampert, B. Schiele, and Z. Akata. Zero-shot learning—a comprehensive evaluation of the good, the bad and the ugly. *IEEE transactions on pattern analysis and machine intelligence*, 41(9):2251–2265, 2018.
 - [51] Y. Xian, T. Lorenz, B. Schiele, and Z. Akata. Feature generating networks for zero-shot learning. In *Proceedings of the IEEE conference on computer vision and pattern recognition*, pages 5542–5551, 2018.
 - [52] Y. Xian, B. Schiele, and Z. Akata. Zero-shot learning—the good, the bad and the ugly. In *Proceedings of the IEEE Conference on Computer Vision and Pattern Recognition*, pages 4582–4591, 2017.
 - [53] J. Zhang, S. Liao, H. Zhang, Y. Long, Z. Zhang, and L. Liu. Data driven recurrent generative adversarial network for generalized zero shot image classification. *Information Sciences*, 625:536–552, 2023.